ЖЭТФ, 2016, том 149, вып. 6, стр. 1249–1259

SPATIAL-SYMMETRY-INDUCED DARK STATES AND CHARGE TRAPPING EFFECTS IN THE COUPLED QUANTUM DOTS

N. S. Maslova [a], ***V. N. Mantsevich*** [a*], ***P. I. Arseev*** [b]

[a] *Lomonosov Moscow State University*
119991, Moscow, Russia

[b] *Lebedev Physical Institute, Russian Academy of Sciences*
119991, Moscow, Russia

Received February 12, 2016

In a system of N interacting single-level quantum dots (QDs) we study relaxation dynamics and current–voltage characteristics determined by symmetry properties of the QD arrangement. Different numbers of dots, initial charge configurations, and various coupling regimes to reservoirs are considered. We reveal that effective charge trapping occurs for particular regimes of coupling to the reservoir when more than two dots form a ring structure with the C_N spatial symmetry. We reveal that the effective charge trapping caused by the C_N spatial symmetry of N coupled QDs depends on the number of dots and the way of coupling to the reservoirs. We demonstrate that the charge trapping effect is directly connected with the formation of dark states, which are not coupled to reservoirs due to the system spatial symmetry C_N. We also reveal the symmetry blockade of the tunneling current caused by the presence of dark states.

DOI: 10.7868/S0044451016060146

1. INTRODUCTION

Recent progress in nanostructuring techniques gives rise to numerous experimental [1–3] and theoretical [4–10] investigations of quantum dot (QD) and quantum dot molecule (QDM) setups with time-dependent parameters [11]. Charges and spins confined in QDs and QDMs are considered attractive components for next-generation optoelectronic devices and quantum information processing because the discrete energy states and properties of confined charges can currently be engineered with structure and composition [12, 13].

Several theoretical methods successfully used in equilibrium were recently extended so as to allow analyzing the dynamics of single QDs and QDMs in out-of-equilibrium states. Some of the proposed methods are mainly analytic [10, 14–16] and others are numerical [17–19]. Nonequilibrium processes in single and coupled QDs were analyzed theoretically by methods such as the Keldysh nonequilibrium Green-function formalism [20], renormalization group theory [21], spin-density-functional theory [22], kinetic Heisenberg equations for local electron density and charge correlation functions [23], or quantum Monte Carlo calculations [24].

Kinetic properties of coupled QDs (QDMs) depend strongly on topology of the dots, which determines energy level spacing and coupling rates [25–27]. Experimental techniques currently allow creating both vertically aligned QDs [7, 10] and lateral QDs [28, 29]. Vertically aligned QDs make it possible to analyse nonstationary effects and formation of various charge and spin configurations. Lateral QDs are considered good candidates for creation of efficient charge traps. Long-lived charge occupation trap states in single QDs were observed experimentally in [30–32]. Single-electron trapping in a double-dot system [33] and extra hole trapping in QDMs [34] have been observed. In [33], the authors measured the temperature of a trapped electron and extracted the tunnel coupling energy by means of charge sensing measurements. A comprehensive configuration-interaction study of a square QD containing several electrons in the presence of an attractive impurity was performed in [35]. The authors revealed that the presence of an impurity significantly changes the charge densities of the two-electron QD excited states. The effect of correlations was revealed in the enhancement of charge density localization within the dot. Two-electron states in a square QD were pro-

* E-mail: vmantsev@gmail.com

posed for the singlet–triplet filtering [36]. The total spin of the initially prepared state localized at the opposite corners of a square QD can be detected by a single charge measurement at the neighboring QD corners. Moreover, coupled square QDs, each including a singlet–triplet qubit, have been proposed as candidates for spin cellular automata for realization of a quantum processor [36]. Instead of a single square QD, one can also use four coupled QDs arranged in a ring. Realization of this proposal requires a rather strong Coulomb interaction of localized electrons to provide only two electrons with opposite spin projections in each square QD. But in such a system, the real space rotational symmetry of coupled QDs is not so important for the suggested realization of qubits. One needs the total symmetry of singlet–triplet states for qubit manipulations. The system of coupled QDs with C_N symmetry can also be a candidate for the realization of individual controlled qubits.

In [34], the authors experimentally measured a single QDM in which one extra hole can be trapped in a metastable higher-energy state of the QDM. The authors also presented a model for the kinetic pathways that lead to the observed dynamic hole trapping. A three-dot trap was considered in [37]. The authors demonstrated how the well-known concept of coherent population trapping in atoms can be transferred to a purely electronic state. A rather complicated scheme was proposed where three dots and reservoirs are connected by reversible and irreversible transitions.

Tunneling current characteristics and the Fano factor in the presence of so-called dark states, connected with the charge trapping effects, were analyzed in [38,39]. In [38], the authors considered a rather complicated QD system that consists of two interacting subsystems — triple QDs with a single excess electron in each subsystem. Dark states appear in such a system only for a particular ratio between charging and exchange energies. In the proposed model, the authors did not consider direct hopping between first and second dots in each subsystem, and hence there was no C_N symmetry in each subsystem and in the entire system. The model under investigation is equivalent to serial triple QDs in parallel configuration. The authors analyzed the tunneling current and the Fano factor depending on the charging Coulomb energy and obtained a suppression of the tunneling current and an increase in the Fano factor when dark states are formed at a particular value of the charging energy. In [39], the authors also analyzed the tunneling current and the Fano factor for a double QD structure (one-level and three-level QDs) depending on the system parameters. In this model, dark states also appear only at a particular ratio between the magnetic energy in the second QD and the s-electron energy in the first QD. Both models [38, 39] require an additional constraint on the system parameters for the appearance of dark states.

The effect of dephasing processes on electron transport through real and artificial atomic chains has been widely discussed during the last decades [40–42]. Tunneling characteristics of linear atomic arrays in the presence of electron–phonon interaction have been studied in detail in [40,43]. A crucial interplay between elastic and inelastic contributions to the phonon-assisted tunneling current and corresponding specific features of tunneling conductivity spectra have been carefully analyzed. Conditions for the enhancement or suppression of the tunneling current caused by interaction with phonons were revealed. In [41], the authors also demonstrated that dephasing can lead to the suppression or enhancement of electron transport in linear triple QDs. Dephasing-assisted transport occurs when the coupling to the drain reservoir exceeds a threshold value. In general, dephasing results in two effects: it destroys dark states in coupled QDs formed due to interference effects, thus enhancing the tunneling current; and it renormalizes the effective tunneling rates to the leads, and therefore the tunneling current can decrease due to the bottleneck effect [41, 44]. The bottleneck effect exists even in a tunneling contact without localized states if a finite relaxation rate of nonequilibrium electrons in the leads is taken into account [44].

Analysis of the time evolution of electron filling numbers in a system of N interacting QDs in the case where only one of the dots is coupled to a reservoir was performed in [23]. The authors demonstrated the presence of strong charge trapping effects in the proposed systems with more than two QDs. Charge trapping in the system of linear QDs can occur at a particular ratio between the relaxation and coupling rates and is a result of the interplay between coherent electron transport and noncoherent irreversible relaxation [45]. But the author of [45] did not focus on the existence of three typical time scales that are responsible for transport dynamics in two coupled QDs [10, 46]. Consequently, the problem of charge trapping in QDs and QDMs is important in condensed matter systems from both the fundamental and technological standpoints, but many aspects of this problem remain unclear.

In this paper, we consider charge relaxation and tunneling current–voltage characteristics in a system of N interacting QDs located in the vertexes of a regular polygon coupled to reservoirs. Different QD numbers, initial charge configurations, and coupling regimes to

the reservoir are analyzed. We demonstrate that effective charge trapping based on the spatial symmetry of $N \geq 3$ coupled QDs depends on the number of dots and the way of coupling to the reservoir. We also reveal a symmetry blockade of the tunneling current and demonstrate the presence of dark and bright states in the proposed system. Dark states appear in the system due to the spatial symmetry and the way of coupling to the reservoirs, and there is no need in any additional constraints on the system parameters (dots energies, hopping amplitudes, and so on).

The considered system makes it possible to form charge traps based on the spatial C_N symmetry of a system of N coupled QDs and to increase the trapping effect for a small number of QDs.

2. THE MODEL

2.1. Time-dependent charge evolution due to sudden switching to the reservoir

We consider relaxation processes in the system of N identical coupled QDs that are located in the vertexes of a regular polygon (Fig. 1*a*). The coupled QDs are weakly connected to the substrate, such that there is no charge transfer from the dots to the substrate. Electron

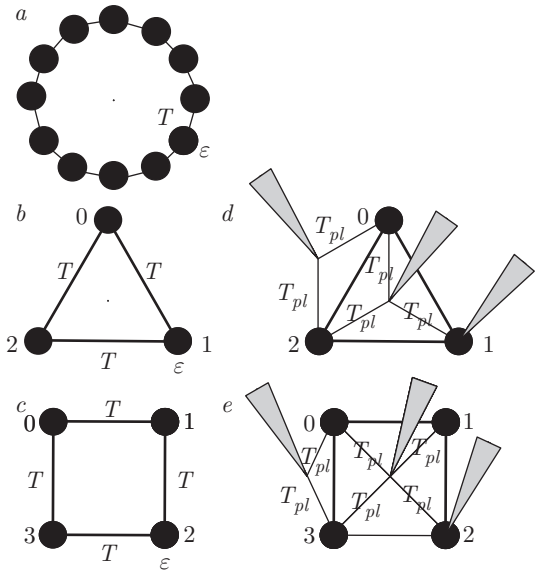

Fig. 1. Schematics of the models: *a*) N coupled single-level QDs with the same energy levels ε; *b*) three coupled single-level QDs; *c*) four coupled single-level QDs. The QD occupations can be measured via the current passing through a nearby quantum point contact capacitively coupled to the dot; *d,e*) schematics of different coupling regimes to the reservoir

coupling is possible only between nearest-neighboring QDs. To minimize the number of free parameters, all the tunnel rates are set equal to T. We assume that the single-particle level spacing in the dots is larger than all the other energy scales, and hence only one spin-degenerate level ε within the QD spectrum is accessible. We consider the case where all energies of single-particle levels in the dots are the same, and therefore inelastic transitions between these levels play no role. We furthermore assume the case where on-site Coulomb repulsion is negligible, and therefore two independent tunneling channels for the electrons with opposite spins are present. The QD system is described by the Hamiltonian

$$\hat{H}_{dots} = \sum_{\sigma,j=0}^{N-1} \varepsilon c_{j\sigma}^{\dagger} c_{j\sigma} + \sum_{\sigma,j\neq j'}^{N-1} T c_{j\sigma}^{\dagger} c_{j'\sigma}, \qquad (1)$$

where we assume the hopping amplitudes T to be independent of momentum and spin, and $c_{j\sigma}^{\dagger}/c_{j\sigma}$ are the creation/annihilation operators of electrons in the QDs. Electronic states in the reservoir are described by the Hamiltonian

$$\hat{H}_{res} = \sum_{\sigma,p} \varepsilon_p c_{p\sigma}^{\dagger} c_{p\sigma}, \qquad (2)$$

where the operators $c_p^{\dagger}/c_p$ correspond to the electron creation/annihilation in reservoir continuous spectrum states (p) with the energy ε_p.

The eigenvalues of the system of N interacting QDs in the absence of coupling to the reservoir, which is described by the Hamiltonian (1), differ for the even and odd number of QDs. For an even number of QDs $[2(k+1) = N]$,

$$\begin{aligned} \lambda_{0,k+1} &= \varepsilon \pm 2T, \\ \lambda_l &= \varepsilon + 2T \cos\frac{\pi l}{k+1}, \end{aligned} \qquad (3)$$

with the index $l = 1, 2, \ldots, k, k+2, \ldots, N-1$. For an odd number of QDs $(2k+1 = N)$,

$$\begin{aligned} \lambda_0 &= \varepsilon + 2T, \\ \lambda_l &= \varepsilon + 2T \cos\frac{2\pi l}{2k+1}, \end{aligned} \qquad (4)$$

with $l = 1, 2, \ldots, N-1$.

Consequently, for an even number of QDs, two nondegenerate energy levels always exist, and all the other energy levels in the spectrum are degenerate. In the case of an odd number of QDs, only one nondegenerate energy level is present, and the other energy levels are doubly degenerate.

Due to the spatial symmetry of the interacting QDs system, Hamiltonian (1) commutes with the rotation

operator $U = \exp(i\varphi_0 l_Z)$, which performs rotation through the angle $\varphi_0 = 2\pi/N$, and therefore the eigenfunctions of the system have the form

$$|\psi_l\rangle = \frac{1}{N^{1/2}} \begin{pmatrix} 1 \\ \exp(i\varphi_0 l) \\ \exp(i\varphi_0 2l) \\ \dots \\ \exp(i\varphi_0 (N-1)l) \end{pmatrix}, \qquad (5)$$

where $l = 0, 1, 2, \dots, N-1$.

The wave functions in the eigenstate basis $|\psi_l\rangle$ can be expressed through the wave functions $|j\rangle$ (a column with the only the jth element equal to unity and all the other elements equal to zero) of the initial QD basis:

$$\begin{aligned} |\psi_l\rangle &= \frac{1}{N^{1/2}} \sum_{j=0}^{N-1} \langle j|\psi_l\rangle |j\rangle = \\ &= \frac{1}{N^{1/2}} \sum_{j=0}^{N-1} \exp(i\varphi_0 jl)|j\rangle, \\ |j\rangle &= \frac{1}{N^{1/2}} \sum_{l=0}^{N-1} \langle \psi_l|j\rangle |\psi_l\rangle = \\ &= \frac{1}{N^{1/2}} \sum_{l=0}^{N-1} \exp(-i\varphi_0 jl)|\psi_l\rangle. \end{aligned} \qquad (6)$$

We now introduce and analyze the results for three different possible experimental realizations of the QD system coupling to the reservoir (for example, the scanning tunneling microscope tip can play the role of the reservoir). The first situation is where the local coupling takes place directly in the center of the regular polygon with the QDs at the vertexes (Fig. 1*d,e*). In this case, all the dots are coupled to the reservoir with the same tunneling amplitude T_p. Tunneling processes in such a system can be described in the QD basis by the Hamiltonian

$$\hat{H}_{tun} = \sum_{\sigma,p,i} T_p c^\dagger_{p\sigma} c_{i\sigma} + T^*_p c^\dagger_{i\sigma} c_{p\sigma}, \qquad (7)$$

where T_p is the tunneling amplitude between QDs and the reservoir. We assume the density of states in the reservoirs ν_0 to be weakly dependent on energy, with the tunneling rate γ_0 defined as $\gamma_0 = \pi\nu_0 T_p^2 N$. When the reservoir is switched to the center of the polygon, we can rewrite the initial QD Hamiltonian (1) and tunneling Hamiltonian (7) in the basis of system eigenstates, taking expression (6) into account:

$$\hat{H} = \sum_{l=0}^{N} \varepsilon_l \psi^+_l \psi_l + \sum_{\sigma,p} N^{1/2} T_p c^\dagger_{p\sigma} \psi_{0\sigma} + T^*_p \psi^+_{0\sigma} c_{p\sigma}. \qquad (8)$$

Tunneling to the reservoir in this system geometry is possible only from the state with $l = 0$ for both odd and even numbers of QDs in the system. Consequently, the system of equations for the time evolution of the electron filling numbers in the basis of QD system eigenstates has the form

$$\begin{aligned} \frac{\partial n_0}{\partial t} &= -\gamma_0 (n_0 - f_p), \\ \frac{\partial n_l}{\partial t} &= 0, \end{aligned} \qquad (9)$$

where f_p is the distribution function for the continuous spectrum states in the reservoir.

Another situation under investigation corresponds to the case where tunneling to the reservoir is possible only from two QDs. Such a situation occurs when the reservoir is situated in the symmetry plane of the segment $[j, j+1]$ between neighboring polygon vertexes outside the polygon (Fig. 1*d,e*). Tunneling processes in this case are described in the QDs basis by the Hamiltonian

$$\begin{aligned} \hat{H}_{tun} = \sum_{\sigma,p} [T_p c^\dagger_{p\sigma} (c_{j\sigma} + c_{j+1\sigma}) + \\ + T^*_p (c^\dagger_{j\sigma} + c^\dagger_{j+1\sigma}) c_{p\sigma}]. \end{aligned} \qquad (10)$$

With the use of expressions (6), we can rewrite initial QD Hamiltonian (1) and tunneling Hamiltonian (10) in the basis of system eigenstates:

$$\hat{H} = \sum_{l=0}^{N-1} \varepsilon_l \psi^+_l \psi_l + \sum_{\sigma,p,l=0}^{N-1} T_{pl} c^\dagger_{p\sigma} \psi_{l\sigma} + T^*_{pl} \psi^+_{l\sigma} c_{p\sigma}, \qquad (11)$$

where

$$T_{pl} = T_p (\exp\{-i\varphi_0 jl\} + \exp\{-i\varphi_0 (j+1)l\}) N^{-1/2}.$$

Consequently, the initial tunneling amplitudes are renormalized in this case and each state has its own tunneling coupling strength with the reservoir T_{pl}. In expressions (6), the wave functions for the initial QD basis $|j\rangle$ contain the operator $c^\dagger_j$, which includes the term $l = k+1$: $\exp(-i\pi j)\psi^+_{k+1} = \pm 1 \psi^+_{k+1}$, and the operator $c^\dagger_{j+1}$, which includes the term $\exp(-i\pi(j+1)) \times$ $\times \psi^+_{k+1} = \mp 1 \psi^+_{k+1}$. Consequently, ψ_{k+1} is not included in the term that describes interaction with the reservoir. Hence, the system of equations for the time evolution of electron filling numbers in the basis of QD system eigenstates in the case where $l \neq k+1$ has the form

$$\begin{aligned} \frac{\partial n_{k+1}}{\partial t} &= 0, \\ \frac{\partial n_l}{\partial t} &= \gamma_l (n_l - f_p), \end{aligned} \qquad (12)$$

where $\gamma_l = \pi\nu_0 T_{pl}^2 N^{-1}$. Therefore, the charge initially present in the state with $l = k + 1$ is fully trapped.

The last situation under investigation deals with tunneling to the reservoir from only one QD j. This situation corresponds to the case where the reservoir is situated directly above a single dot in the polygon vertex (Fig. 1*d,e*). Tunneling processes in the QD basis are described by the Hamiltonian

$$\hat{H}_{tun} = \sum_{\sigma,p} T_p c_{p\sigma}^\dagger c_{j\sigma} + T_p^* c_{j\sigma}^\dagger c_{p\sigma}. \qquad (13)$$

With the use of expressions (6), we can rewrite initial QDs Hamiltonian (1) and tunneling Hamiltonian (13) in the basis of system eigenstates,

$$\hat{H} = \sum_{l=0}^{N-1} \varepsilon_l \psi_l^+ \psi_l + \sum_{\sigma,p,l=0}^{N} T'_{pl} c_{p\sigma}^\dagger \psi_{l\sigma} + T_{pl}^{'*} \psi_{l\sigma}^+ c_{p\sigma}, \quad (14)$$

where $T'_{pl} = T_p \exp(-i\varphi_0 jl) N^{-1/2}$. Consequently, the tunneling amplitudes are renormalized in this case, but each state ψ_l is coupled to the reservoir with the relaxation rate γ_l. The system of equations for the time evolution of electron filling numbers in the basis of QD system eigenstates has the form

$$\frac{\partial n_l}{\partial t} = \gamma'_l (n_l - f_p), \qquad (15)$$

where $\gamma'_l = \pi\nu_0 T_{pl}^{'2}$. Consequently, charge trapping does not occur in the coupled QD system in this case.

Because we are interested in specific features of the nonstationary time evolution of the initially localized charge in coupled QDs, we consider the situation where the condition $(\varepsilon - \varepsilon_F)/\gamma \gg 1$ is fulfilled. Our investigations deal with the low-temperature regime when the Fermi level is well defined and the temperature is much lower than all typical relaxation rates in the system. Consequently, the distribution function of electrons in the leads (band electrons) is a Fermi step. For simplicity in what follows, we consider charge relaxation processes in the system of three (odd) and four (even) QDs. The obtained results for different initial charge configurations and different coupling regimes to the reservoir in the cases of three and four interacting QDs are discussed in Sec. 3.

2.2. Nonequilibrium tunneling current in the presense of a second reservoir

We also consider the situation where the system of QDs is situated between two leads of a tunneling contact. All planar QDs are directly coupled to the substrate (its "own" reservoir) (Fig. 2*a*), which is considered as one of the leads, and therefore charge transfer

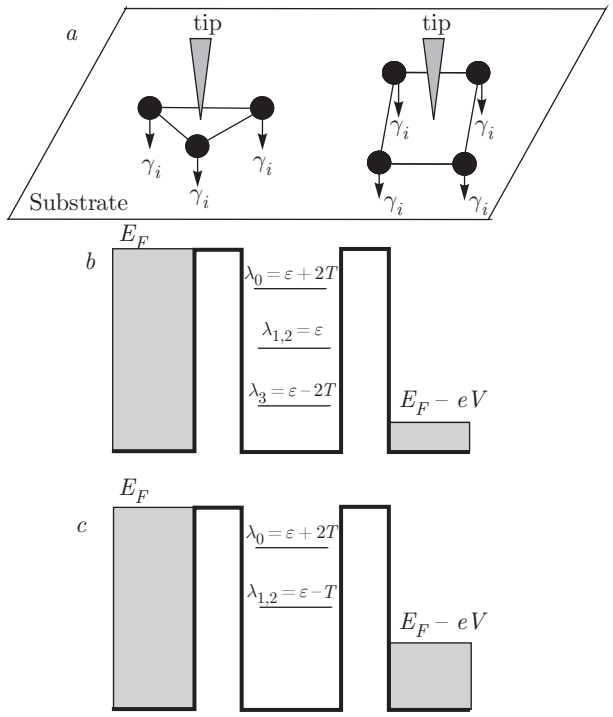

Fig. 2. *a*) Schematics of the QD localization between two leads of a tunneling contact, the substrate and the tip; *b,c*) Schematics of dark and bright states for four and three dots in the system respectively

to the substrate is allowed. Another lead is formed due to the coupling with the scanning tunneling microscope (STM) tip, which is switched to the system at $t = 0$.

Electronic states in the reservoirs are now described by the Hamiltonian

$$\hat{H}_{res} = \sum_{\sigma,p} (\varepsilon_p - eV) c_{p\sigma}^\dagger c_{p\sigma} + \sum_{\sigma,k} \varepsilon_k c_{k\sigma}^\dagger c_{k\sigma}, \qquad (16)$$

where the operators $c_{p(k)}^\dagger / c_{p(k)}$ correspond to electron creation/annihilation in the reservoir continuous spectrum states ($p(k)$) with the energy $\varepsilon_{p(k)}$; eV is the applied tip bias voltage.

Tunneling processes in such a system can be described in the QD eigenstate basis by the Hamiltonian

$$\hat{H}_{tun} = \sum_{\sigma,p,l} T_{pl} c_{p\sigma}^\dagger c_{l\sigma} + T_{pl}^* c_{l\sigma}^\dagger c_{p\sigma} + \\ + \sum_{\sigma,k,l} T_{kl} c_{k\sigma}^\dagger c_{l\sigma} + T_{kl}^* c_{l\sigma}^\dagger c_{k\sigma}, \quad (17)$$

where $T_{p(k)l}$ are the tunneling transfer amplitudes between the eigenstate l of the QD system and the reservoirs. If the density of states in the reservoirs ν_0 is weakly dependent on energy, the tunneling rate $\gamma_{p(k)l}$ is defined as $\gamma_{p(k)l} = \pi\nu_0 T_{p(k)l}^2$.

The tunneling current–voltage characteristics and stationary occupation of QDs now depend on the way of coupling to both reservoirs. We first focus on the case where the second reservoir (the STM tip) is locally switched to the center of the regular polygon with the QDs in vertexes. In this case, only one bright state exists in the system ($l = 0$), which contributes to the tunneling current due to the C_N spatial symmetry of the system (the system of coupled QDs returns to itself under rotation through the angle $2\pi/N$). The energy of this eigenstate is $\lambda_0 = \varepsilon + 2T$. All other eigenstates with energies λ_l are decoupled from the second reservoir ($T_{pl} = 0$, $l \neq 0$) and are therefore dark states (see Fig. 2*b,c*), which do not contribute to the tunneling current. These dark states directly correspond to the states where charge trapping occurs in the relaxation problem.

At the initial instant $t = 0$, the electron occupation numbers n_l are stationary equilibrium filling numbers, which are determined by interaction with the first reservoir (the substrate with $E_F = 0$):

$$n_l(0) = n_l^{st} = \frac{1}{\pi}\int d\omega\, f_k(\omega)\frac{\gamma_{kl}}{(\omega-\lambda_l)^2+\gamma_{kl}^2}, \quad (18)$$

where $f_k(\omega)$ is the Fermi distribution function. When the second lead is switched to the center of the regular polygon, the state with $l = 0$ acquires an additional tunneling rate γ_{p0}, and hence the width of the eigenenergy level λ_0 changes to $\gamma_0 = \gamma_{k0} + \gamma_{p0}$. For the QD eigenstates with $l \neq 0$, the widths of energy levels λ_l and the tunneling rates γ_{kl} remain unchanged ($\gamma_l = \gamma_{kl} + \gamma_{pl}$ with $\gamma_{pl} = 0$). Consequently, for $t > 0$, the occupation numbers with $l \neq 0$ are determined by the expressions

$$n_l(t) = n_l(0) = n_l^{st}. \quad (19)$$

The time-dependent occupation $n_0(t)$ can be found from the nonstationary Keldysh Green's function [10]

$$\begin{aligned} n_0(t) = n_0^{st}\exp(-2\gamma_0 t) + \frac{1}{\pi}\frac{\gamma_{k0}}{\gamma_0}\times \\ \times\int d\omega\, f_k(\omega)\frac{\gamma_0}{(\omega-\lambda_0)^2+\gamma_0^2}\times \\ \times\left(1+\exp(-2\gamma_0 t)-2\cos((\omega-\lambda_0)t)\exp(-\gamma_0 t)\right)+ \\ +\frac{1}{\pi}\frac{\gamma_{p0}}{\gamma_0}\int d\omega\, f_p(\omega)\frac{\gamma_0}{(\omega-\lambda_0)^2+\gamma_0^2}\times \\ \times\left(1+\exp(-2\gamma_0 t)-2\cos((\omega-\lambda_0)t)\exp(-\gamma_0 t)\right), \quad (20) \end{aligned}$$

where $\gamma_0 = \gamma_{k0} + \gamma_{p0}$.

For $t \to \infty$, the stationary occupation of the state n_0^{st} changes to $\widetilde{n}_0^{st}$ due to the coupling to the second reservoir:

$$\begin{aligned} \widetilde{n}_0^{st} = \frac{1}{\pi}\frac{\gamma_{k0}}{\gamma_0}\int d\omega\, f_k(\omega)\frac{\gamma_0}{(\omega-\lambda_0)^2+\gamma_0^2}+ \\ +\frac{1}{\pi}\frac{\gamma_{p0}}{\gamma_0}\int d\omega\, f_p(\omega)\frac{\gamma_0}{(\omega-\lambda_0)^2+\gamma_0^2}. \end{aligned}$$

Even for a zero applied bias ($eV = 0$), $\widetilde{n}_0^{st}$ differs from n_0^{st} due to the energy level width changing. The tunneling current through the system is determined as

$$I = \sum_l \int d\omega\, 4\gamma_{pl}\,\mathrm{Im}\, G_{ll}(\omega)(n_l(\omega) - f_p(\omega)), \quad (21)$$

where [47]

$$\mathrm{Im}\, G_{ll}(\omega) = \frac{\gamma_l}{(\omega-\lambda_l)^2+(\gamma_l)^2}.$$

States with $l \neq 0$ do not contribute to the tunneling current ($\gamma_{pl} = 0$) and are therefore dark states. The state with $l = 0$ determines the tunneling current

$$I = \int d\omega\, \frac{4\gamma_{k0}\gamma_{p0}}{\gamma_0}\,\mathrm{Im}\, G_{00}(\omega)(f_k(\omega) - f_p(\omega)). \quad (22)$$

When the second reservoir is switched to a single dot in the polygon vertex (Fig. 1*d,e*), all the eigenstates λ_l contribute to the tunneling current, which is determined by the standard expression

$$I = \sum_l \int d\omega\, \frac{4\gamma_{kl}\gamma_{pl}}{\gamma_l}\,\mathrm{Im}\, G_{ll}(\omega)(f_k(\omega) - f_p(\omega)). \quad (23)$$

In this case, there are no dark states in the system. This is because a renormalization of the tunneling amplitudes occurs and each state ψ_l is coupled to the reservoir with its own relaxation rate γ_l and charge trapping is absent in the proposed system geometry.

When the tip is situated in the symmetry plane of the segment $[j, j+1]$ between neighboring polygon vertexes outside the polygon, only one dark state appears for an even ($N = 2(k+1)$) number of QDs. The eigenstate with $l = k+1$ is a dark state, which does not contribute to the tunneling current. Due to the C_N spatial symmetry of the system, wave functions for the initial QD basis $|j\rangle$ contain the operator $c_j^\dagger$, which includes the term $l = k+1$, $\exp(-i\pi j)\psi_{k+1}^+ = \pm 1\psi_{k+1}^+$, and the operator $c_{j+1}^\dagger$, which includes the term $\exp(-i\pi(j+1))\psi_{k+1}^+ = \mp 1\psi_{k+1}^+$. Consequently, ψ_{k+1} is not included in the term that describes interaction with the reservoir.

Current–voltage characteristics for different ways of coupling to the second reservoir are depicted in Fig. 6 and are discussed in the next section.

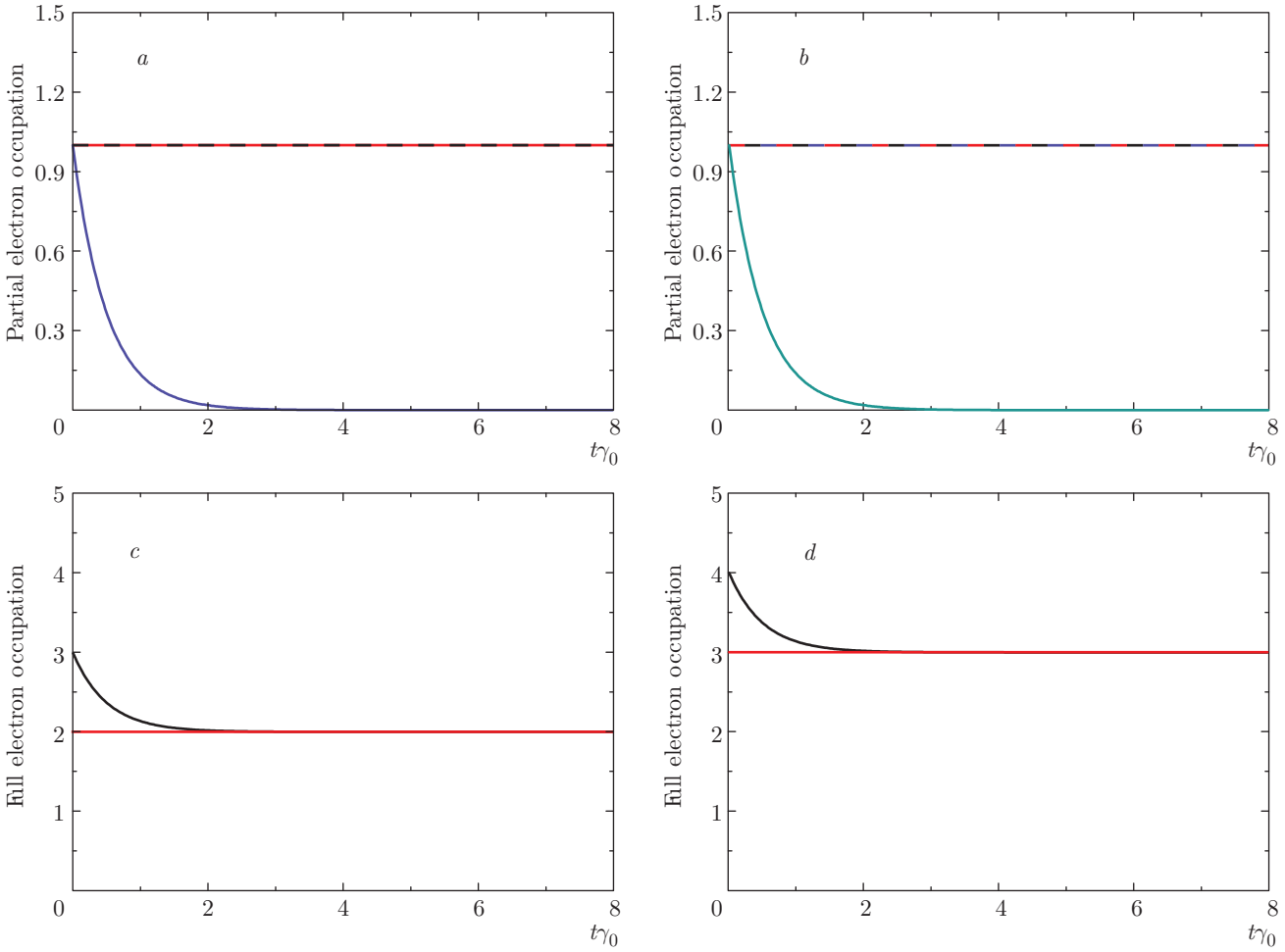

Fig. 3. (Color online) Time evolution of the electron filling numbers (occupancies) in the case of three (a,c) and four (b,d) interacting QDs when local coupling takes place directly in the center of the regular polygon with the QDs in vertexes. a and b demonstrate time evolution of partial filling numbers in the case where all the system eigenstates are initially occupied. c and d demonstrate time evolution of the full filling numbers in the case where all system eigenstates are initially occupied (black line) and when the highest state with $l = 0$ is initially unoccupied (red line). The parameters $\varepsilon_j/\gamma_0 = 2.5$, $T/\gamma_0 = 1.5$, $\gamma_0 = 1$, and $\gamma_{l\neq 0} = 0$ are the same for all the figures; $\varphi_0 = \pi/3$ and $\varphi_0 = \pi/2$ for three and four dots respectively

3. RESULTS AND DISCUSSION

Time evolution of the electron filling numbers strongly depends on the initial charge configuration and the way of coupling to the reservoir. The behavior of partial and full occupancies of the coupled QD system states obtained for three and four QDs is depicted in Figs. 3–5. We first consider the situation where local coupling takes place directly in the center of the regular polygon with the QDs in the vertexes (Fig. 1d,e). In this case, all the dots are coupled to the reservoir with the same tunneling amplitudes (see Fig. 3). For this geometry, tunneling to the reservoir is possible only from the state with the highest energy $\varepsilon + 2T$ ($l = 0$) for both an odd (three, the blue line in Fig. 2a) and an even (four, the green line in Fig. 3b) number of QDs in the system due to expressions (8) and (9). The charge localized initially in the system states with lower energies — the double-degenerate state with the energy $\varepsilon - T$ in the case of three QDs (see the black dashed and red lines in Fig. 3a) and the double-degenerate state with the energy ε and a nondegenerate state with the energy $\varepsilon - 2T$ in the case of four QDs (see the black dashed, blue dotted, and red lines in Fig. 3b) — is trapped in these states. The trapping effect in the considered system geometry is the result of the QD system symmetry, which results in the tunneling only from the state with $l = 0$.

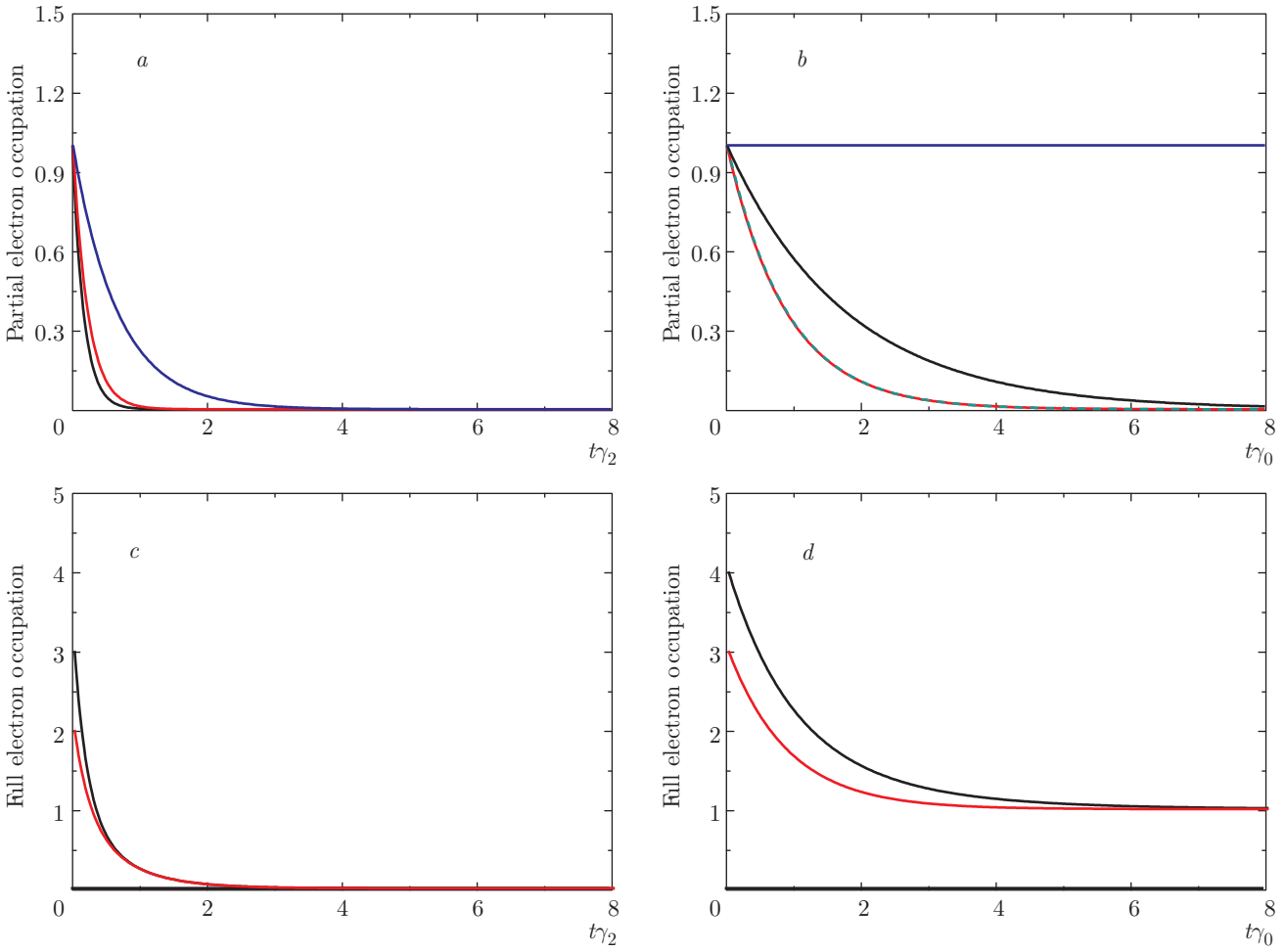

Fig. 4. (Color online) Time evolution of the electron filling numbers (occupancies) in the case of three (a,c) and four (b,d) interacting QDs when tunneling to the reservoir is possible only from two QDs. a and b demonstrate time evolution of partial filling numbers in the case where all system eigenstates are initially occupied. c and d demonstrate time evolution of the full filling numbers in the case where all system eigenstates are initially occupied (black line) and when the highest state with $l = 0$ is initially unoccupied (red line). The parameters and relaxation rates for three dots are $\varepsilon_j/\gamma_2 = 3.3$, $T/\gamma_2 = 2$, $\gamma_0/\gamma_2 = 4$, $\gamma_1/\gamma_2 = 3$, and $\gamma_2 = 0.75$. The parameters and relaxation rates for four dots are $\varepsilon_j/\gamma_0 = 4.45$, $T/\gamma_0 = 2.6$, $\gamma_0 = 0.56$, $\gamma_1/\gamma_0 = 2$, $\gamma_2/\gamma_0 = 0$, and $\gamma_3/\gamma_0 = 2$. $\varphi_0 = \pi/3$ and $\varphi_0 = \pi/2$ for three and four dots respectively

The full system occupancies are shown in Fig. 3c and Fig. 3d for three and four dots. The situation where all the energy states are occupied at the initial instant is shown in Fig. 3c,d by black lines. The full occupancy time evolution depicted by the red line corresponds to the case where at the initial instant the system state with the highest energy $\varepsilon + 2T$ is empty and all the lower energy states are fully occupied. It is evident that charge trapping is present in both cases. All charge is trapped in the system when only lower energy states are occupied at the initial instant. When all the system states are occupied at the initial instant, the electron filling numbers undergo relaxation to the reservoir, but the full system occupancy reaches a constant value when the charge localized in the state with the highest energy becomes empty. In both cases, the trapped charge amplitudes acquire the same value.

We now discuss the situation where tunneling to the reservoir is possible only from two QDs, which happens when the reservoir is situated in the symmetry plane of the segment $[j, j+1]$ between neighboring polygon vertexes outside the polygon (see Fig. 4 and Fig. 1d,e). Due to expressions (11) and (12) in the case where the considered QD system contains an odd (three) number of dots, the charge trapping effect does not exist (see Fig. 4a,c) and each state demonstrates the initially lo-

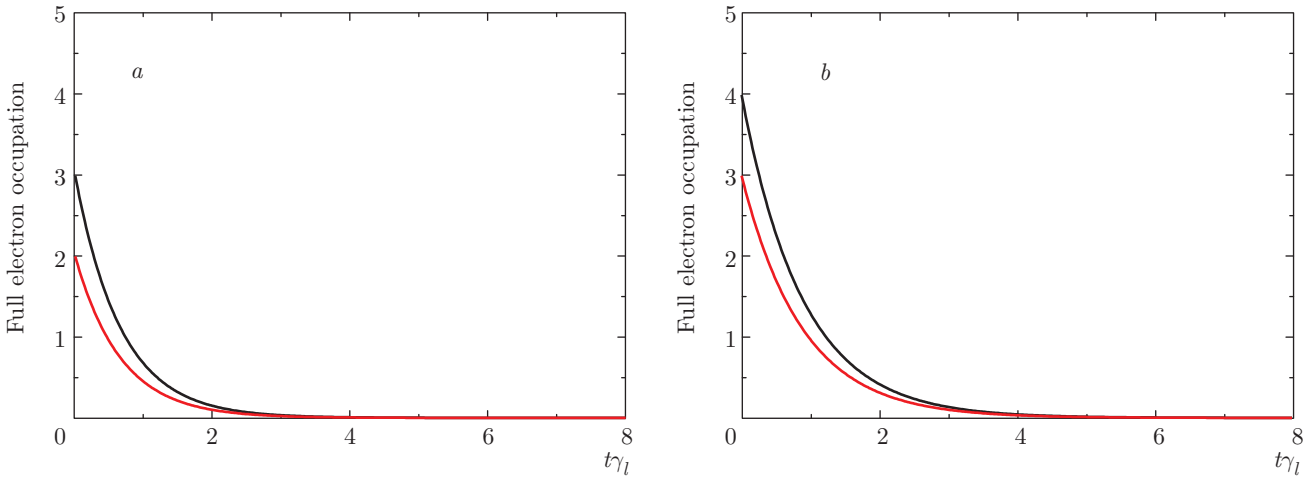

Fig. 5. (Color online) Time evolution of the full electron filling numbers (occupancies) in the case of three (a) and four (b) interacting QDs when tunneling to the reservoir is possible only from one QD in the case where all system eigenstates are initially occupied (black lines) and when the highest state with $l = 0$ is initially unoccupied (red lines). The parameters and partial relaxation rates for three dots are $\varepsilon_j/\gamma_l = 3.3$, $T/\gamma_l = 2$, and $\gamma_l = 0.75$. The parameters and partial relaxation rates for four dots are $\varepsilon_j/\gamma_l = 4.45$, $T/\gamma_l = 2.6$, and $\gamma_l = 0.56$. $\varphi_0 = \pi/3$ and $\varphi_0 = \pi/2$ for three and four dots respectively

calized charge relaxation with its own tunneling coupling strength caused by renormalization of the initial tunneling amplitudes (see Fig. 4*a*). The nondegenerate state has a larger relaxation rate than double-degenerate states (see the black line in the Fig. 4*a*).

The charge trapping effect arises for an even (four) number of QDs (see Fig. 4*b*,*d*). If all system states are occupied at the initial instant, charge trapping takes place only for the nondegenerate lowest-energy state $\varepsilon - 2T$ (see the blue line in Fig. 4*b*). All other system states demonstrate charge relaxation to the reservoir. Double-degenerate states with the energy ε exhibit relaxation with the same rates (see the green dashed and red lines in Fig. 4*b*). The highest nondegenerate state has a lower relaxation rate than the double-degenerate states (see the black line in Fig. 4*b*). The charge trapping effect is well pronounced for the time evolution of full occupancies (see Fig. 4*c*,*d*) when all the system states are occupied at the initial instant and when the charge localized in the state with the highest energy level is initially empty.

The situation where tunneling to the reservoir takes place from only one QD is rather trivial (Fig. 1*d*,*e*). Expressions (14) and (15) demonstrate that tunneling to the reservoir from all the states occurs for both an odd and an even number of QDs in the case where all system eigenstates are initially occupied (black lines in Fig. 5) and when the highest state with $l = 0$ is initially unoccupied (red lines in Fig. 5). Consequently, charge trapping does not exist. The full system occupancies in the case where all the energy states are occupied at the initial instant are shown in Fig. 5 for three and four dots.

Typical current–voltage characteristics for different types of coupling to the second reservoir for the system of three and four QDs are shown in Fig. 6. The direct manifestation of the appearance of dark states in the case where the second reservoir is coupled to the center of the polygon is the presence of only one step in the current–voltage characteristic, which corresponds to the bright state eigenenergy value λ_0 (the black lines in Fig. 6). On the other hand, when the second reservoir is connected to a vertex of the polygon, all the eigenstates λ_l contribute to the tunneling current. We can clearly see well-pronounced steps in the current–voltage characteristic for the applied bias equal to the eigenstate energies λ_l (the red dashed line in Fig. 6). When the second reservoir is switched in the symmetry plane of the segment $[j, j+1]$ for four QDs, the step corresponding to $eV = \varepsilon - 2T$ (dark state energy) is absent in the current–voltage characteristic. For an odd number of QDs, there are no dark states for such a way of switching to the reservoir (the blue lines in Fig. 6).

We note that the same value of the on-site Coulomb repulsion in QDs in the Hartree approximation (we consider identical QDs) does not disturb the spatial C_N symmetry and, consequently, the proposed system behavior is then the same.

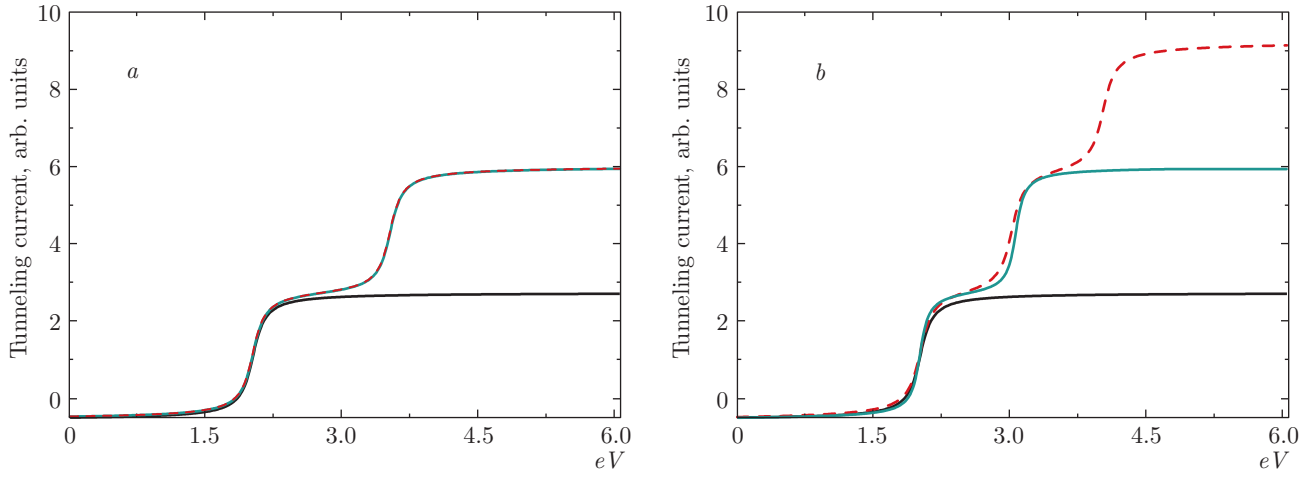

Fig. 6. (Color online) Tunneling current through the system of three (a) and four (b) QDs. The black line corresponds to the case where the second reservoir is switched directly above the center of the regular polygon. The red dashed line corresponds to the case where the second reservoir is switched directly above a single dot in the regular polygon vertex. The blue line corresponds to the case where the second reservoir is switched in the symmetry plane of the segment $[j, j+1]$. The system parameters are $\varepsilon = 2$ and $T = 0.5$ for three QDs and $\varepsilon = 3$ and $T = 0.5$ for four QDs. The tunneling contact is considered to be symmetric: $\gamma_{kl} = \gamma_{pl}$

4. CONCLUSION

We analyzed the relaxation dynamics and current–voltage characteristics in a system of N interacting QDs situated in the vertexes of a regular polygon, coupled to reservoirs. Different numbers of QDs, different initial charge configurations, and different coupling regimes to the reservoir were analyzed. We demonstrated that the system symmetry results in the presence of double-degenerate and nondegenerate eigenstates in the system spectrum. The number of nondegenerate eigenstates differs in the cases of even and odd number of QDs. We revealed that effective charge trapping caused by the C_N spatial symmetry of coupled QDs depends on the number of QDs and the way of switching to the reservoir. The obtained charge trapping effect is directly connected with the formation of dark states, which are not coupled to the reservoir due to the system spatial symmetry C_N.

Charge trapping is always present and is most effective when coupling to the reservoir occurs in the center of the polygon because tunneling to the reservoir is possible only from a single state with $l = 0$. When the reservoir is located in the symmetry plane of the segment $[j, j+1]$ between neighboring polygon vertexes outside the polygon, trapping is possible only for an even number of QDs in the system. Only for an even number of dots there exists an eigenenergy state that is not involved in the interaction processes between QDs and the reservoir. Charge is not trapped when the reservoir is coupled only to a single dot.

We also revealed a symmetry blockade of the tunneling current. Tunneling characteristics of the QD system with the C_N spatial symmetry are also determined by the way of coupling to both reservoirs. It is possible that the eigenstate of an isolated QD system is bright for one of the reservoirs and dark for the other. The tunneling current flowing through such a state is impossible, even though the occupation of this state depends on the value of the applied bias. Such a state occupation can be changed due to tunneling transitions to one of the reservoirs, but it does not contribute to the tunneling current flowing through the whole QD system. The presence of such states does not result in additional peculiarities in the current–voltage characteristic. Hence, a symmetry blockade of the tunneling current occurs.

This paper was supported by the RFBR (grants №№ 16-32-60024mol-a-dk, 14-02-00434).

REFERENCES

1. W. G. van der Wiel, S. De Franceschi, J. M. Elzerman et al., Rev. Mod. Phys. **75**, 1 (2002).

2. R. M. Potok, I. G. Rau, H. Shtrikman et al., Nature **446**, 167 (2007).

3. T. Hayashi, T. Fujisawa, H. D. Cheong, Y. H. Jeong, and Y. Hirayama, Phys. Rev. Lett. **91**, 226804 (2003).

4. C. A. Stafford and S. Das Sarma, Phys. Rev. Lett. **72**, 3590 (1994).

5. K. A. Matveev, L. I. Glazman, and H. U. Baranger, Phys. Rev. B **54**, 5637 (1996).

6. D. Boese, W. Hofstetter, and H. Schoeller, Phys. Rev. B **66**, 125315 (2002).

7. K. Kikoin and Y. Avishai, Phys. Rev. B **65**, 115329 (2002).

8. P. A. Orellana, G. A. Lara, and E. V. Anda, Phys. Rev. B **65**, 155317 (2002).

9. P. I. Arseyev, N. S. Maslova, and V. N. Mantsevich, Sol. St. Comm. **152**, 1545 (2012).

10. P. I. Arseyev, N. S. Maslova, and V. N. Mantsevich, Europ. Phys. J. B **85**(7), 249 (2012).

11. R. Hanson, L. P. Kouwenhoven, J. R. Petta, S. Tarucha, and L. M. K. Vandersypen, Rev. Mod. Phys. **79**, 1217 (2007).

12. F. H. L. Koppens, J. A. Folk, J. M. Elzerman et al., Science **309**, 1346 (2005).

13. M. F. Doty, J. I. Climente, M. Korkusinski et al., Phys. Rev. Lett. **102**, 047401 (2009).

14. A. Hackl, D. Roosen, S. Kehrein, and W. Hofstetter, Phys. Rev. Lett. **102**, 196601 (2009).

15. M. Pletyukhov, D. Schuricht, and H. Schoeller, Phys. Rev. Lett. **104**, 106801 (2010).

16. H. Schoeller and J. Konig, Phys. Rev. Lett. **84**, 3686 (2000).

17. F. B. Anders and A. Schiller, Phys. Rev. B **74**, 245113 (2006).

18. P. Schmitteckert, Phys. Rev. B **70**, 121302 (2004).

19. F. Heidrich-Meisner, A. E. Feiguin, and E. Dagotto, Phys. Rev. B **79**, 235336 (2009).

20. L. V. Keldysh, Sov. Phys. JETP **20**, 1018 (1964).

21. K. Kikoin and Y. Avishai, Phys. Rev. Lett. **86**, 2090 (2001).

22. S. M. Reimann and M. Manninen, Rev. Mod. Phys. **74**, 1283 (2002).

23. V. N. Mantsevich, N. S. Maslova, and P. I. Arseyev, Sol. St. Comm. **168**, 36 (2013).

24. W. M. C. Foulkes, L. Mitas, R. J. Needs et al., Rev. Mod. Phys. **73**, 33 (2001).

25. M. A. Kastner, Rev. Mod. Phys. **64**, 849 (1992).

26. C. W. J. Beenakker, Phys. Rev. B **44**, 1646 (1991).

27. Y. Alhassid, Rev. Mod. Phys. **72**, 895 (2000).

28. M. A. Kastner, Phys. Today **46**(1), 24 (1993).

29. R. C. Ashoori, Nature **379**, 413 (1996).

30. M. Kuno, D. P. Fromm, H. F. Hamann et al., J. Chem. Phys. **112**, 3117 (2000).

31. M. Kuno, D. P. Fromm, H. F. Hamann et al., J. Chem. Phys. **115**, 1028 (2001).

32. M. R. Hummon, A. J. Stollenwerk, V. Narayanamurti et al., Phys. Rev. B **81**, 115439 (2010).

33. M. Pioro-Ladriere, M. R. Abolfath, P. Zawadzki et al., Phys. Rev. B **72**, 125307 (2005).

34. W. Liu, A. S. Bracker, D. Gammon, and M. F. Doty, Phys. Rev. B **87**, 195308 (2013).

35. B. S. Pujari, K. Joshi, D. G. Kanhere, and S. A. Blundell, Phys. Rev. B **78**, 125414 (2008).

36. A. Bayat, C. E. Creffield, J. H. Jefferson, M. Pepper, and S. Bose, Semicond. Sci. Techol. **30**, 105025 (2015).

37. B. Michaelis, C. Emary, and C. W. J. Beenakker, Europhys. Lett. **73**, 677 (2006).

38. C. Poltl, C. Emary, and T. Brandes, Phys. Rev. B **87**, 045416 (2013).

39. C. Emary, C. Poltl, and T. Brandes, Phys. Rev. B **80**, 235321 (2009).

40. C. Caroli, R. Combescot, D. Lederer-Rozenblatt, P. Nozières, and D. Saint-James, Phys. Rev. B **12**, 3977 (1975).

41. L. D. Contreras-Pulido, M. Bruderer, S. F. Huelga, and M. B. Plenio, New J. Phys. **16**, 113061 (2014).

42. Y. N. Chen, T. Brandes, C. M. Li, and D. S. Chuu, Phys. Rev. B **69**, 245323 (2004).

43. P. I. Arseev and N. S. Maslova, Phys. Uspekhi **53**, 1151 (2010).

44. P. I. Arseev and N. S. Maslova, JETP **102**, 1056 (1992).

45. S. A. Gurvitz, Phys. Rev. B **57**, 6602 (1998).

46. P. I. Arseyev, N. S. Maslova, and V. N. Mantsevich, JETP Lett. **95**, 521 (2012).

47. V. N. Mantsevich and N. S. Maslova, Sol. St. Comm. **150**, 2072 (2010).